

Topological Micromotion of Floquet Quantum Systems

Peng Xu,¹ Wei Zheng,^{2,3,*} and Hui Zhai^{1,†}

¹*Institute for Advanced Study, Tsinghua University, Beijing 100084, China*

²*Hefei National Laboratory for Physical Sciences at the Microscale and Department of Modern Physics, University of Science and Technology of China, Hefei 230026, China*

³*CAS Center for Excellence in Quantum Information and Quantum Physics, University of Science and Technology of China, Hefei 230026, China*

(Dated: March 1, 2022)

The Floquet Hamiltonian has often been used to describe a time-periodic system. Nevertheless, because the Floquet Hamiltonian depends on a micro-motion parameter, the Floquet Hamiltonian with a fixed micro-motion parameter cannot faithfully represent a time-periodic system, which manifests as the anomalous edge states. Here we show that an accurate description of a Floquet system requires a set of Hamiltonian spanning all values of the micro-motion parameter, and this micro-motion parameter can be viewed as an extra synthetic dimension of the system. Therefore, we show that a d -dimensional Floquet system can be described by a $d + 1$ -dimensional static Hamiltonian, and the advantage of this representation is that the periodic boundary condition is automatically imposed along the extra-dimension, which enables a straightforward definition of topological invariants. The topological invariant in the $d + 1$ -dimensional system can ensure a $d - 1$ -dimensional edge state of the d -dimensional Floquet system. Here we show two examples where the topological invariant is defined as the three-dimensional Hopf invariant. We highlight that our scheme of classifying Floquet topology on the micro-motion space is different from the previous classification of Floquet topology on the time space.

I. INTRODUCTION

Studying periodically driven quantum systems, which are also referred to as Floquet systems, has become a major research topic in the frontier of quantum matters¹⁻⁴. Periodic driving can be realized, for instance, by illuminating a solid-state material with an electromagnetic wave⁵⁻⁸ or by modulating optical lattices depth⁹⁻¹² or interaction strengths¹³⁻¹⁸ in ultracold atomic gases. Floquet engineering can simulate synthetic gauge fields^{16,19-30}, and create novel phases such as topologically nontrivial states³¹⁻³⁸ and discrete time crystals³⁹⁻⁴³. It can also realize interesting quantum dynamics such as prethermalization⁴³⁻⁵³ and many-body echo⁵⁴⁻⁵⁶.

The Floquet Hamiltonian is a popular tool to describe a periodically driven system. The key idea of the Floquet Hamiltonian is to effectively describe a time-periodic system by a time-independent Hamiltonian^{2,3,57,58}. Considering a time-periodic Hamiltonian $\hat{H}(t)$ with $\hat{H}(t) = \hat{H}(t + T)$, we can define a Floquet effective Hamiltonian \hat{H}_F as ($\hbar = 1$)

$$e^{-i\hat{H}_F(\alpha_1)T} = \hat{\mathcal{T}}e^{-i\int_{\alpha_1/\omega}^{(2\pi+\alpha_1)/\omega} \hat{H}(t)dt}, \quad (1)$$

where $\omega = 2\pi/T$, $\hat{\mathcal{T}}$ is the time-ordering operator, and α_1/ω is the initial time. Therefore, if an observer only makes observations at integer periods of time $t = (\frac{\alpha_1}{2\pi} + n)T$, this observer cannot distinguish whether the evolution is governed by $\hat{H}(t)$ or $\hat{H}_F(\alpha_1)$. In Floquet engineering, one can properly design the driving scheme so that the Floquet Hamiltonian can display intriguing properties, such as exhibiting nontrivial topology and novel dynamics.

However, if another observer makes observations at a different set of times $t = (\frac{\alpha_2}{2\pi} + n)T$, the corresponding time evolution should be governed by

$$e^{-i\hat{H}_F(\alpha_2)T} = \hat{\mathcal{T}}e^{-i\int_{\alpha_2/\omega}^{(2\pi+\alpha_2)/\omega} \hat{H}(t)dt}. \quad (2)$$

Now let us use $\hat{U}(\alpha_2, \alpha_1)$ to denote a unitary transformation

$$\hat{U}(\alpha_2, \alpha_1) = \hat{\mathcal{T}}e^{-i\int_{\alpha_1/\omega}^{\alpha_2/\omega} \hat{H}(t)dt}, \quad (3)$$

it is easy to see that

$$e^{-i\hat{H}_F(\alpha_1)T} = \hat{U}^\dagger(\alpha_2, \alpha_1)e^{-i\hat{H}_F(\alpha_2)T}\hat{U}(\alpha_2, \alpha_1). \quad (4)$$

Therefore, $\hat{H}_F(\alpha)$ with different α are equivalent up to a unitary transformation, i.e.,

$$\hat{H}_F(\alpha_1) = \hat{U}^\dagger(\alpha_2, \alpha_1)\hat{H}_F(\alpha_2)\hat{U}(\alpha_2, \alpha_1). \quad (5)$$

The $\hat{U}(\alpha_2, \alpha_1)$ connects observations at two time slots within one period T , and is also known as the *micro-motion*^{2,3}. That is to say, although $\hat{H}_F(\alpha)$ with different α share the same set of eigenenergies, their eigenstates differ by a unitary transformation $\hat{U}(\alpha_2, \alpha_1)$. Hence, the conclusion is that $\hat{H}_F(\alpha)$ with a fixed α cannot provide a faithful representation of this time-periodic system. As a physical manifestation of this statement, there exists situations that $\hat{H}_F(\alpha)$ is topologically trivial but the system exhibits topologically stable edge states, which are known as the anomalous edge states. Such anomalous edge states have been explained in terms of the winding numbers of the evolution operator⁵⁹⁻⁶¹ and higher order topology⁶², and have been experimentally realized in various systems⁶³⁻⁶⁵.

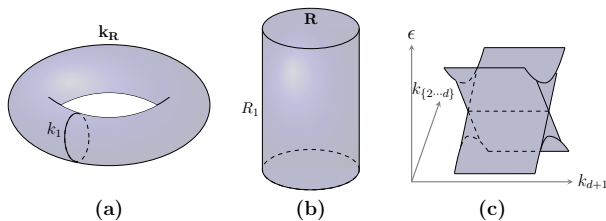


FIG. 1: (a) The Hamiltonian set $\{\hat{H}_F(k_1, \dots, k_d, \alpha), \alpha \in [0, 2\pi]\}$ can be viewed as a Hamiltonian in $\hat{H}(k_1, \dots, k_d, k_{d+1})$ in $(d+1)$ -dimension. Here \mathbf{k}_R denotes $\{k_2, \dots, k_{d+1}\}$. (b) A real space geometry for the $(d+1)$ -dimensional system, with open boundary condition in one of the spatial dimension denoted by R_1 and periodic boundary condition in the rest dimensions denoted by $\mathbf{R} = \{R_2, \dots, R_{d+1}\}$. (c) Schematic of energy dispersion for systems shown in (b), as a function of good quantum numbers k_2, k_3, \dots, k_{d+1} . This dispersion is flat along k_{d+1} direction.

Therefore, a proper description of the anomalous edge states requires complete information beyond $\hat{H}_F(\alpha)$ with a fixed α . Previous approaches involve the evolution operator $\hat{U}(t)$ at all time instead of integer periods of time, and $\hat{U}(t)$ is defined as

$$\hat{U}(t) = \hat{\mathcal{T}} e^{-i \int_0^t \hat{H}(t) dt}. \quad (6)$$

However, it is easy to see that, although $\hat{H}(t)$ is periodic in t , $\hat{U}(t)$ is not. In other word, $\hat{U}(0) \neq \hat{U}(T)$ and the evolution operator is not periodic along the time direction. Hence, an extra operation is designed to impose periodicity in t such that the topological invariant can be well defined^{59–61}.

In this work, we propose an alternative scheme that, instead of studying $\hat{H}_F(\alpha)$ with a fixed α or $\hat{U}(t)$, an effective Hamiltonian set $\{\hat{H}_F(\alpha), \alpha \in [0, 2\pi]\}$ provides complete information for a time-periodic system. Intuitively, this is because for a given α , the Hamiltonian $\hat{H}_F(\alpha)$ correctly reproduces observations made at $t = (\frac{\alpha}{2\pi} + n)T$. Hence, with all $\alpha \in [0, 2\pi]$, observations made at any time t can be properly captured. Moreover, the advantage of our scheme is that $\hat{H}(\alpha)$ is naturally periodic in terms of the parameter α . As one can easily see from Eq. (1), $\hat{H}_F(0) = \hat{H}_F(2\pi)$. Therefore, the topological invariant can be straightforwardly defined. Here we will utilize this view to characterize the topology of a non-interacting band, and we will show that this description can properly capture the anomalous edge states.

II. GENERAL THEORY.

Let us consider a d -dimensional time-periodic Hamiltonian $\hat{H}(k_1, \dots, k_d, t)$, and the corresponding effective Hamiltonian set is $\{\hat{H}_F(k_1, \dots, k_d, \alpha), \alpha \in [0, 2\pi]\}$. Since the effective Hamiltonian is periodic in α , it is therefore quite natural to consider α as an extra momentum

component denoted by k_{d+1} . Thus, this Hamiltonian set is replaced by a Hamiltonian in $(d+1)$ -dimension as $\hat{H}(k_1, \dots, k_d, k_{d+1})$, as shown in Fig. 1(a). Now we denote \mathbf{k}_R as $\{k_2, \dots, k_{d+1}\}$, and their corresponding real space coordinates are denoted by $\mathbf{R} = \{R_2, \dots, R_{d+1}\}$. When we apply an open boundary condition along R_1 , and keep periodic boundary condition along other directions, \mathbf{R} spans the surface on the edge of the system, as shown in Fig. 1(b). The bulk-edge correspondence states that, if the Hamiltonian $\hat{H}(k_1, \dots, k_{d+1})$ possesses a nontrivial topological invariant, the system hosts in-gap surface states localized in the surfaces spanned by \mathbf{R} , and the dispersion of the in-gap states as a function of the good quantum number \mathbf{k}_R is schematically shown in Fig. 1(c). A specific feature is that the dispersion is flat along k_{d+1} direction, since the Hamiltonians with different k_{d+1} (i.e., α) are equivalent up to unitary transformations. Thus, if such surface states exist, their dispersion in terms of $\{k_2, \dots, k_d\}$ should be identical for arbitrary fixed k_{d+1} . That is to say, the Floquet Hamiltonian $\hat{H}_F(\alpha)$ with a fixed α also displays in-gap edge states when taking open boundary condition along R_1 . This discussion shows that the topological invariant in the $(d+1)$ -dimensional Hamiltonian $\hat{H}(k_1, \dots, k_{d+1})$ can protect $(d-1)$ -dimensional edge states in the d -dimensional time-periodic Hamiltonian $\hat{H}(k_1, \dots, k_d, t)$. Since the physical meaning of the extra dimension comes from the micro-motion of the Floquet system, we term it as “*topological micro-motion*”.

Here we should note that the possible topological phase in $\hat{H}(k_1, \dots, k_{d+1})$ is strongly constrained by the fact that the Hamiltonians with different k_{d+1} are connected by unitary transformations and the band dispersion is flat along k_{d+1} . This constraint rules out the edge states of $\hat{H}(k_1, \dots, k_{d+1})$ being Dirac type.

III. TOPOLOGICAL HOPF MICRO-MOTION

Here we consider a two-dimensional two-band time-periodic system $\hat{H}(k_1, k_2, t)$, and the Floquet effective Hamiltonian is given by $\hat{H}_F(k_1, k_2, \alpha)$. Viewing α as k_3 , the eigenstates of the three-dimensional Hamiltonian are generally written as $|\varphi_{\mathbf{k}}\rangle$ with $\hat{H}_F(\mathbf{k})|\varphi_{\mathbf{k}}\rangle = \epsilon_{\mathbf{k}}|\varphi_{\mathbf{k}}\rangle$, where $\mathbf{k} = (k_1, k_2, k_3)$. We can then introduce a pseudo-spin direction $\mathbf{n}(\mathbf{k}) = \langle \varphi_{\mathbf{k}} | \sigma | \varphi_{\mathbf{k}} \rangle$. Therefore, we define a mapping from the three-dimensional momentum space \mathbf{k} to the Bloch sphere \mathbf{n} , $f : \mathbf{k} \rightarrow \mathbf{n}$. The topology of such a mapping can be classified by the homotopy group $\pi_3(S^2) = \mathbb{Z}$, and the corresponding topological invariant can be described by the Hopf invariant^{66–68}. Considering two different directions in the Bloch sphere denoted by \mathbf{n}_1 and \mathbf{n}_2 , the inverse images $f^{-1}(\mathbf{n}_1)$ and $f^{-1}(\mathbf{n}_2)$ are respectively two trajectories in the three-dimensional momentum space. The Hopf invariant can actually be described by the linking number of these two trajectories, and this linking number is independent of the choices of

\mathbf{n}_1 and \mathbf{n}_2 . More details of the definition and the calculation of the Hopf invariant is presented in the Appendix. A nontrivial Hopf invariant can protect edge states in the two-dimensional surface of a three-dimensional insulator, known as the Hopf insulator.^{66–68} With the general theory discussed above, we will show that the Hopf invariant of the three-dimensional Floquet Hamiltonian $\hat{H}_F(k_1, k_2, \alpha)$ can also protect one-dimensional edge states in the two-dimensional time-periodic system $\hat{H}(k_1, k_2, t)$.

IV. EXAMPLES

Below, we demonstrate this result with two examples. Especially, we will show that in these two cases, $\hat{H}_F(k_1, k_2, \alpha)$ with a fixed α is always a topologically trivial Hamiltonian, but can still process in-gap edge states with open boundary condition. Thus, the edge states in these cases are the anomalous edge states. In both cases, we see a definite correlation between the Hopf invariant in $\hat{H}_F(k_1, k_2, k_3)$ and the presence of stable edge states in time-periodic system $\hat{H}(k_1, k_2, t)$.

Example I. In the first example, we consider a time-periodic two-band Hamiltonian

$$\hat{H} = \begin{cases} \hat{H}_1, & nT < t \leq nT + t_0 \\ \hat{H}_2, & nT + t_0 < t \leq (n+1)T \end{cases}. \quad (7)$$

The two-band Hamiltonian can be written as $\mathbf{h}(\mathbf{k}) \cdot \sigma$, where $h_x = \sin k_x$, $h_y = \sin k_y$ and $h_z = \mu + \cos(k_x) + \cos(k_y) + \cos(k_x)\cos(k_y)$. We take $\hat{H}_1 = \mathbf{h}(\mathbf{k}) \cdot \sigma$ with $\mu < -3$ or $\mu > 1$, such that \hat{H}_1 is always topologically trivial. \hat{H}_2 is chosen as $\epsilon_0 \mathbf{h}(\mathbf{k}) \cdot \sigma / |\mathbf{h}(\mathbf{k})|$, such that the band dispersion of \hat{H}_2 is always flat. For \hat{H}_2 , we can choose the parameter μ to make \hat{H}_2 either topologically trivial or nontrivial. However, since \hat{H}_2 has a flat band dispersion, and by choosing $\epsilon_0 = \pi / (T - t_0)$, \hat{H}_2 always contributes an identity to the evolution operator after one time period. Thus, the effective Hamiltonian is determined by \hat{H}_1 along, and it is easy to see that, for $\alpha = 0$, the Floquet Hamiltonian is always given by $\hat{H}_F(0) = t_0 \hat{H}_1 / T$, which is definitely a trivial one. This also means that all \hat{H}_F are topologically trivial because they are equivalent up to unitary transformations.

In this model, it can be shown that when \hat{H}_2 is topologically trivial or nontrivial, the corresponding $\hat{H}_F(\mathbf{k})$ respectively has a zero or non-zero linking number in the three-dimensional momentum space, and such examples are shown in Fig. 2(a) and (c). This is because, according to Eq. (5), $\hat{H}_F(\alpha)$ with different α are connected by a unitary transformation $\hat{U}^\dagger(\alpha_2, \alpha_1)$, and therefore, the eigenstates of $\hat{H}_F(\alpha)$ with different α are also connected by the same unitary transformation. In this case, it maps the problem to a dynamical quench problem under Hamiltonian either \hat{H}_1 or \hat{H}_2 . It is known from the previous studies of the quench problem that whether a

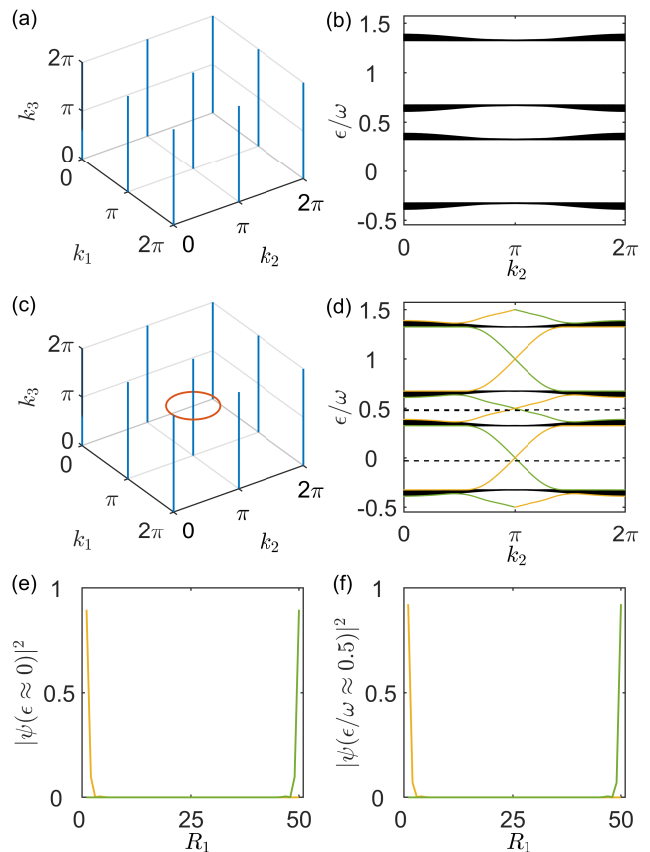


FIG. 2: Linking number (a, c), spectrum (b, d) and edge states (e, f) of Model I. (a, c) The inverse images of the south (blue straight lines) and the north (red circle) poles of the three-dimensional Hamiltonian $\hat{H}_F(k_1, k_2, k_3)$. (b, d) the spectrum for two-dimensional Floquet effective Hamiltonian $\hat{H}_F(k_1, k_2, \alpha)$ with a fixed α . Here we have fixed $\mu = -10$ in \hat{H}_1 for all plots. We have chosen $\mu = -5$ for \hat{H}_2 such that \hat{H}_2 is a topologically trivial case in (a) and (b), and $\mu = -2$ such that \hat{H}_2 is a topologically nontrivial case for (c) and (d). (e, f) The real space distribution of the edge states correspond to the in-gap states shown in (d), with quasi-energies located at zero-energy (e) and energy π/T (f) respectively. Here t_0 is chosen as 0.1.

linking number exists depends on whether \hat{H}_2 is topologically nontrivial or not⁶⁹.

In Fig. 2(b) and (d), we compute the spectrum of the two-dimensional effective Hamiltonian with open boundary condition along R_1 direction. We can see that when a nontrivial \hat{H}_2 leads to a non-zero linking number in the three-dimensional space, the edge states are present along the one-dimensional edge of the Floquet system. The edge states are present in both the energy window around zero and around π/T . At the same edge, two edge states at different energies have the same chirality. Therefore, back-scatterings are forbidden at the same edge, which ensures the stability of these edge states.

In this model, it is also interesting to ask how the physics recovers the limit $t_0 \rightarrow T$. On one hand, as long

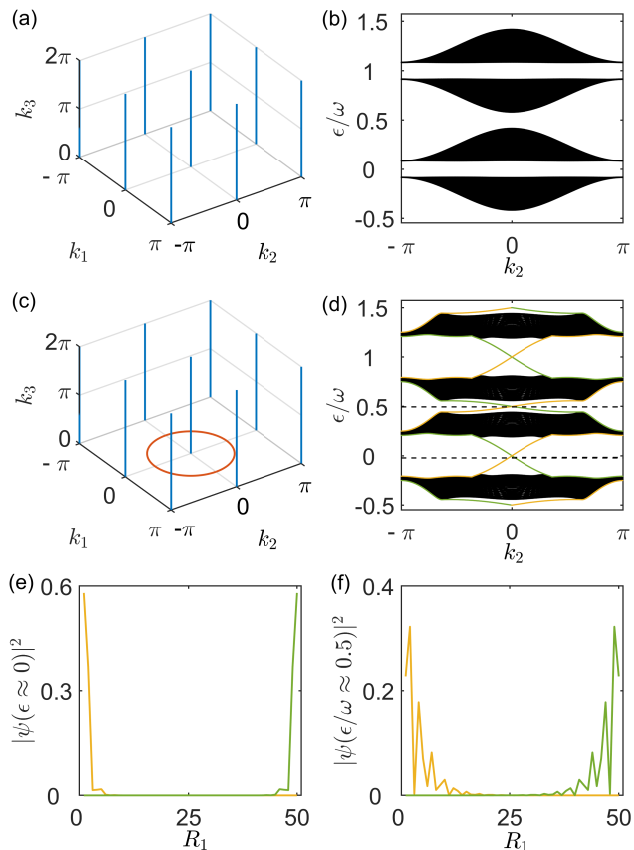


FIG. 3: Linking number (a, c), spectrum (b, d) and edge states (e, f) of Model II. (a, c) The inverse images of the south (blue straight lines) and the north (red circle) poles of the three-dimensional Hamiltonian $\hat{H}_F(k_1, k_2, k_3)$. (b, d) the spectrum for two-dimensional Floquet effective Hamiltonian $\hat{H}_F(k_1, k_2, \alpha)$ with a fixed α . Here we have chosen $\mu = -10$ and $\omega = 12$ in (a) and (b), and $\mu = -2$ and $\omega = 4$ for (c) and (d). (e, f) The real space distribution of the edge states correspond to the in-gap states shown in (d), with quasi-energies located at zero-energy (e) and energy π/T (f) respectively.

as \hat{H}_2 is nontrivial, the above discussion always results in a non-zero linking number, which is independent of the choice of t_0 , and this further leads to the conclusion that the edge states are always present for any $0 < t_0 < T$. On the other hand, taking the limit $t_0 \rightarrow T$, the Floquet system returns to a time-independent system governed by a topologically trivial Hamiltonian \hat{H}_1 and no edge state should exist. To resolve this paradox, we find that the localization length of the edge states increases as t_0 increases. Eventually, when $t_0 \rightarrow T$, states localized at two opposite edges meet in the bulk and gap out each other.

Example II. In this example, we consider a time-dependent Hamiltonian

$$\hat{H} = \mathbf{h}(\mathbf{k}) \cdot \boldsymbol{\sigma} + \sigma_z \cos(\omega t), \quad (8)$$

where $\mathbf{h}(\mathbf{k})$ is the same as described in the Example I and is time-independent. Here we can also choose different

μ such that $\mathbf{h}(\mathbf{k}) \cdot \boldsymbol{\sigma}$ can be either trivial or nontrivial, and this time-independent part gives rise to two static band dispersions $\epsilon_{\pm}(\mathbf{k}) = \pm|h(\mathbf{k})|$. The $\sigma_z \cos(\omega t)$ term couples the static dispersions to the Floquet sidebands, which shifts $\epsilon_{\pm}(\mathbf{k})$ by $\pm\omega$ as $\epsilon_{\pm}(\mathbf{k}) \mp \omega$.

In Fig. 3(a) and (b), we consider the situation that the static bands are topologically trivial, and we choose a large ω such that the static bands do not overlap with the Floquet sidebands. In this case, the Floquet bands are still topologically trivial and there are no edge states. In Fig. 3(c) and (d), we consider another situation that the static bands are topologically nontrivial, and therefore, two bands with dispersion $\pm|h(\mathbf{k})|$ have opposite topological numbers. Then we choose a proper ω such that a static band (say, band with dispersion $|h(\mathbf{k})|$) will overlap with another Floquet sideband (say, band with dispersion $-|h(\mathbf{k})| + \omega$). In this case, in-gap edge states occur but the resulting Floquet bands are topologically trivial, because the mixed two bands originally have opposite topological numbers, and the band inversion will cancel their topological invariants.

In Fig. 3(a) and (c), we show the linking numbers of $\hat{H}_F(k_1, k_2, k_3)$. We can see that the linking number in the three-dimensional space is respectively zero or non-zero for the situations that the edge states are absent or present. Same as the Example I, when the edge states are present, they appear in both energy window around zero and around π/T and have the same chirality at the same edge, as shown in Fig. 3(e) and (f).

V. CONCLUSION AND DISCUSSION

In summary, we point out that the Floquet effective Hamiltonian of a d -dimensional system periodically depends on a micro-motion parameter α , and the effective Hamiltonian set with all α faithfully presents all information of a Floquet system. Taking α as another synthetic dimension, we view the effective Hamiltonian set with α as a Hamiltonian defined in $(d+1)$ -dimension. For a non-interacting band insulator, we show that the topological number of this $(d+1)$ -dimensional Hamiltonian directly protects stable $(d-1)$ -dimensional edge states of the d -dimensional Floquet system⁷⁰. Here we would like to highlight again the difference between this work and the existing works on the Floquet topology^{59–61,71–74}. The difference is that here we classify the topology in $\mathbf{k} - \alpha$ space and the existing works all classify the topology in $\mathbf{k} - t$ space. As concrete examples, we discuss the situations where a three-dimensional Hopf invariant can lead to the anomalous edge states. We have explicitly shown two examples and this theory can also be applied to recent experiments on anomalous Floquet topological insulator⁶⁵, where the anomalous edge states in the experimental models can also be attributed to the Hopf invariant. We note that the Hopf invariant is limited to two-band models, and future works are needed for generalizing to higher band cases. Finally, we expect that

this $(d + 1)$ -dimensional Hamiltonian can also help us to understand other phenomena in Floquet systems such as Floquet discrete time crystal.

Acknowledgment. This work is supported by Beijing Outstanding Young Scientist Program and NSFC Grant No. 11734010.

Appendix A: The Definition of the Hopf Invariant

For a two-band model, the Hamiltonian can be written as

$$\hat{H} = \mathbf{h}(\mathbf{k}) \cdot \boldsymbol{\sigma}. \quad (\text{A1})$$

The groundstate of the Hamiltonian (A1) can be denoted as

$$\varphi(\mathbf{k}) = \begin{pmatrix} \varphi_1(\mathbf{k}) \\ \varphi_2(\mathbf{k}) \end{pmatrix}, \quad (\text{A2})$$

from which we can define a pseudo-spin direction $\mathbf{n}(\mathbf{k}) = \varphi(\mathbf{k})^\dagger \boldsymbol{\sigma} \varphi(\mathbf{k})$. The Hopf invariant of the Hamiltonian (A1) can be evaluated by the integral form ⁷⁵

$$\text{Hopf} = - \int d^3\mathbf{k} (\mathbf{j} \cdot \mathbf{A}), \quad (\text{A3})$$

where the local current $j^\mu = \frac{1}{8\pi} \epsilon^{\mu\nu\lambda} \mathbf{n} \cdot (\partial_\nu \mathbf{n} \times \partial_\lambda \mathbf{n})$, and \mathbf{A} satisfies $\nabla \times \mathbf{A} = \mathbf{j}$. Note that A_μ is defined up to the gauge freedom $A_\mu \rightarrow A_\mu - \partial_\mu \Lambda$. Under the gauge choice $\partial^\mu A_\mu = 0$, we have $A_\mu = i\varphi^\dagger \partial_\mu \varphi$. Numerically, we first calculate the ground states $\varphi(\mathbf{k})$ of the effective Floquet Hamiltonian $\hat{H}_F(\mathbf{k} = (k_1, k_2, \alpha))$ at each momentum \mathbf{k} , with which $\mathbf{n}(\mathbf{k})$ can be obtained. Secondly, we calculate the local current $j^\mu(\mathbf{k})$ and gauge field $A_\mu(\mathbf{k})$. Finally, the Hopf invariant can be obtained directly according to the definition Eq. (A3).

-
- * Electronic address: zw8796@ustc.edu.cn
† Electronic address: lzhai@tsinghua.edu.cn
- ¹ M. Bukov, L. D'Alessio, and A. Polkovnikov, *Adv. Phys.* **64**, 139 (2015).
 - ² A. Eckardt and E. Anisimovas, *New J. Phys.* **17**, 093039 (2015).
 - ³ A. Eckardt, *Rev. Mod. Phys.* **89**, 011004 (2017).
 - ⁴ T. Oka and S. Kitamura, *Annu. Rev. Condens. Matter Phys.* **10**, 387 (2019).
 - ⁵ A. Kimel, A. Kirilyuk, P. Usachev, R. Pisarev, A. Balbashov, and T. Rasing, *Nature* **435**, 655 (2005).
 - ⁶ D. Fausti, R. Tobey, N. Dean, S. Kaiser, A. Dienst, M. C. Hoffmann, S. Pyon, T. Takayama, H. Takagi, and A. Cavalleri, *Science* **331**, 189 (2011).
 - ⁷ M. Mitrano, A. Cantaluppi, D. Nicoletti, S. Kaiser, A. Perucchi, S. Lupi, P. Di Pietro, D. Pontiroli, M. Riccò, S. R. Clark, et al., *Nature* **530**, 461 (2016).
 - ⁸ Y. Han, X.-Q. Luo, T.-F. Li, W. Zhang, S.-P. Wang, J. Tsai, F. Nori, and J. You, *Phys. Rev. Applied* **11**, 014053 (2019).
 - ⁹ N. Gemelke, E. Sarajlic, Y. Bidel, S. Hong, and S. Chu, *Phys. Rev. Lett.* **95**, 170404 (2005).
 - ¹⁰ H. Lignier, C. Sias, D. Ciampini, Y. Singh, A. Zenesini, O. Morsch, and E. Arimondo, *Phys. Rev. Lett.* **99**, 220403 (2007).
 - ¹¹ C. Sias, H. Lignier, Y. P. Singh, A. Zenesini, D. Ciampini, O. Morsch, and E. Arimondo, *Phys. Rev. Lett.* **100**, 040404 (2008).
 - ¹² C. V. Parker, L.-C. Ha, and C. Chin, *Nat. Phys.* **9**, 769 (2013).
 - ¹³ S. E. Pollack, D. Dries, R. G. Hulet, K. M. F. Magalhães, E. A. L. Henn, E. R. F. Ramos, M. A. Caracanhas, and V. S. Bagnato, *Phys. Rev. A* **81**, 053627 (2010).
 - ¹⁴ L. W. Clark, L.-C. Ha, C.-Y. Xu, and C. Chin, *Phys. Rev. Lett.* **115**, 155301 (2015).
 - ¹⁵ L. W. Clark, A. Gaj, L. Feng, and C. Chin, *Nature* **551**, 356 (2017).
 - ¹⁶ L. W. Clark, B. M. Anderson, L. Feng, A. Gaj, K. Levin, and C. Chin, *Phys. Rev. Lett.* **121**, 030402 (2018).
 - ¹⁷ A. Behrle, T. Harrison, J. Kombe, K. Gao, M. Link, J.-S. Bernier, C. Kollath, and M. Köhl, *Nat. Phys.* **14**, 781 (2018).
 - ¹⁸ J. H. V. Nguyen, M. C. Tsatsos, D. Luo, A. U. J. Lode, G. D. Telles, V. S. Bagnato, and R. G. Hulet, *Phys. Rev. X* **9**, 011052 (2019).
 - ¹⁹ M. Aidelsburger, M. Atala, S. Nascimbène, S. Trotzky, Y.-A. Chen, and I. Bloch, *Phys. Rev. Lett.* **107**, 255301 (2011).
 - ²⁰ J. Struck, C. Ölschläger, M. Weinberg, P. Hauke, J. Simonet, A. Eckardt, M. Lewenstein, K. Sengstock, and P. Windpassinger, *Phys. Rev. Lett.* **108**, 225304 (2012).
 - ²¹ M. Aidelsburger, M. Atala, M. Lohse, J. T. Barreiro, B. Paredes, and I. Bloch, *Phys. Rev. Lett.* **111**, 185301 (2013).
 - ²² J. Struck, M. Weinberg, C. Ölschläger, P. Windpassinger, J. Simonet, K. Sengstock, R. Höppner, P. Hauke, A. Eckardt, M. Lewenstein, et al., *Nat. Phys.* **9**, 738 (2013).
 - ²³ H. Miyake, G. A. Siviloglou, C. J. Kennedy, W. C. Burton, and W. Ketterle, *Phys. Rev. Lett.* **111**, 185302 (2013).
 - ²⁴ M. Atala, M. Aidelsburger, M. Lohse, J. T. Barreiro, B. Paredes, and I. Bloch, *Nat. Phys.* **10**, 588 (2014).
 - ²⁵ S. Greschner, G. Sun, D. Poletti, and L. Santos, *Phys. Rev. Lett.* **113**, 215303 (2014).
 - ²⁶ F. Görg, K. Sandholzer, J. Minguzzi, R. Desbuquois, M. Messer, and T. Esslinger, *Nat. Phys.* **15**, 1161 (2019).
 - ²⁷ C. Schweizer, F. Grusdt, M. Berngruber, L. Barbiero, E. Demler, N. Goldman, I. Bloch, and M. Aidelsburger, *Nat. Phys.* **15**, 1168 (2019).
 - ²⁸ L. Barbiero, C. Schweizer, M. Aidelsburger, E. Demler, N. Goldman, and F. Grusdt, *Sci. Adv.* **5**, eaav7444 (2019).
 - ²⁹ W. Zheng and P. Zhang, arXiv:2011.01500 (2020).
 - ³⁰ P. Xu, T.-S. Deng, W. Zheng, and H. Zhai, *Phys. Rev. A* **103**, L061302 (2021).
 - ³¹ T. Oka and H. Aoki, *Phys. Rev. B* **79**, 081406 (2009).
 - ³² N. H. Lindner, G. Refael, and V. Galitski, *Nat. Phys.* **7**, 490 (2011).

- ³³ M. C. Rechtsman, J. M. Zeuner, Y. Plotnik, Y. Lumer, D. Podolsky, F. Dreisow, S. Nolte, M. Segev, and A. Szameit, *Nature* **496**, 196 (2013).
- ³⁴ W. Zheng and H. Zhai, *Phys. Rev. A* **89**, 061603 (2014).
- ³⁵ G. Jotzu, M. Messer, R. Desbuquois, M. Lebrat, T. Uehlinger, D. Greif, and T. Esslinger, *Nature* **515**, 237 (2014).
- ³⁶ M. Aidelsburger, M. Lohse, C. Schweizer, M. Atala, J. T. Barreiro, S. Nascimbène, N. Cooper, I. Bloch, and N. Goldman, *Nat. Phys.* **11**, 162 (2015).
- ³⁷ J. W. McIver, B. Schulte, F.-U. Stein, T. Matsuyama, G. Jotzu, G. Meier, and A. Cavalleri, *Nat. Phys.* **16**, 38 (2020).
- ³⁸ L. Zhang, L. Zhang, and X.-J. Liu, *Phys. Rev. Lett.* **125**, 183001 (2020).
- ³⁹ D. V. Else, B. Bauer, and C. Nayak, *Phys. Rev. Lett.* **117**, 090402 (2016).
- ⁴⁰ N. Y. Yao, A. C. Potter, I.-D. Potirniche, and A. Vishwanath, *Phys. Rev. Lett.* **118**, 030401 (2017).
- ⁴¹ J. Zhang, P. Hess, A. Kyprianidis, P. Becker, A. Lee, J. Smith, G. Pagano, I.-D. Potirniche, A. C. Potter, A. Vishwanath, et al., *Nature* **543**, 217 (2017).
- ⁴² S. Choi, J. Choi, R. Landig, G. Kucsko, H. Zhou, J. Isoya, F. Jelezko, S. Onoda, H. Sumiya, V. Khemani, et al., *Nature* **543**, 221 (2017).
- ⁴³ J. Rovny, R. L. Blum, and S. E. Barrett, *Phys. Rev. Lett.* **120**, 180603 (2018).
- ⁴⁴ D. A. Abanin, W. De Roeck, and F. Huvneers, *Phys. Rev. Lett.* **115**, 256803 (2015).
- ⁴⁵ T. Mori, T. Kuwahara, and K. Saito, *Phys. Rev. Lett.* **116**, 120401 (2016).
- ⁴⁶ D. Abanin, W. De Roeck, W. W. Ho, and F. Huvneers, *Commun. Math. Phys.* **354**, 809 (2017).
- ⁴⁷ D. A. Abanin, W. De Roeck, W. W. Ho, and F. Huvneers, *Phys. Rev. B* **95**, 014112 (2017).
- ⁴⁸ D. V. Else, B. Bauer, and C. Nayak, *Phys. Rev. X* **7**, 011026 (2017).
- ⁴⁹ J. Rovny, R. L. Blum, and S. E. Barrett, *Phys. Rev. B* **97**, 184301 (2018).
- ⁵⁰ A. Rubio-Abadal, M. Ippoliti, S. Hollerith, D. Wei, J. Rui, S. L. Sondhi, V. Khemani, C. Gross, and I. Bloch, *Phys. Rev. X* **10**, 021044 (2020).
- ⁵¹ W. Beatriz, O. Janes, A. Akkiraju, A. Pillai, A. Oddo, P. Reshetikhin, E. Druga, M. McAllister, M. Elo, B. Gilbert, et al., arXiv:2104.01988 (2021).
- ⁵² P. Peng, C. Yin, X. Huang, C. Ramanathan, and P. Capellaro, *Nat. Phys.* **17**, 444 (2021).
- ⁵³ A. Kyprianidis, F. Machado, W. Morong, P. Becker, K. S. Collins, D. V. Else, L. Feng, P. W. Hess, C. Nayak, G. Pagano, et al., *Science* **372**, 1192 (2021).
- ⁵⁴ Y.-Y. Chen, P. Zhang, W. Zheng, Z. Wu, and H. Zhai, *Phys. Rev. A* **102**, 011301 (2020).
- ⁵⁵ C. Lv, R. Zhang, and Q. Zhou, *Phys. Rev. Lett.* **125**, 253002 (2020).
- ⁵⁶ Y. Cheng and Z.-Y. Shi, arXiv:2004.12754 (2020).
- ⁵⁷ N. Goldman and J. Dalibard, *Phys. Rev. X* **4**, 031027 (2014).
- ⁵⁸ N. Goldman, J. Dalibard, M. Aidelsburger, and N. R. Cooper, *Phys. Rev. A* **91**, 033632 (2015).
- ⁵⁹ T. Kitagawa, E. Berg, M. Rudner, and E. Demler, *Phys. Rev. B* **82**, 235114 (2010).
- ⁶⁰ M. S. Rudner, N. H. Lindner, E. Berg, and M. Levin, *Phys. Rev. X* **3**, 031005 (2013).
- ⁶¹ F. Nathan and M. S. Rudner, *New J. Phys.* **17**, 125014 (2015).
- ⁶² S. Franca, F. Hassler, and I. C. Fulga, *SciPost Phys. Core* **4**, 007 (2021).
- ⁶³ S. Mukherjee, A. Spracklen, M. Valiente, E. Andersson, P. Öhberg, N. Goldman, and R. R. Thomson, *Nat. Commun.* **8**, 1 (2017).
- ⁶⁴ L. J. Maczewsky, J. M. Zeuner, S. Nolte, and A. Szameit, *Nat. Commun.* **8**, 1 (2017).
- ⁶⁵ K. Wintersperger, C. Braun, F. N. Ünal, A. Eckardt, M. Di Liberto, N. Goldman, I. Bloch, and M. Aidelsburger, *Nat. Phys.* **16**, 1058 (2020).
- ⁶⁶ J. E. Moore, Y. Ran, and X.-G. Wen, *Phys. Rev. Lett.* **101**, 186805 (2008).
- ⁶⁷ D.-L. Deng, S.-T. Wang, C. Shen, and L.-M. Duan, *Phys. Rev. B* **88**, 201105 (2013).
- ⁶⁸ R. Kennedy, *Phys. Rev. B* **94**, 035137 (2016).
- ⁶⁹ C. Wang, P. Zhang, X. Chen, J. Yu, and H. Zhai, *Phys. Rev. Lett.* **118**, 185701 (2017).
- ⁷⁰ A different manifestation of such topological micromotion has been discussed in J. C. Budich, Y. Hu, and P. Zoller, *Phys. Rev. Lett.* **118**, 105302 (2017).
- ⁷¹ R. Roy and F. Harper, *Phys. Rev. B* **96**, 155118 (2017).
- ⁷² T. Schuster, S. Gazit, J. E. Moore, and N. Y. Yao, *Phys. Rev. Lett.* **123**, 266803 (2019).
- ⁷³ F. N. Ünal, A. Eckardt, and R.-J. Slager, *Phys. Rev. Research* **1**, 022003 (2019).
- ⁷⁴ A. Gómez-León and G. Platero, *Phys. Rev. Lett.* **110**, 200403 (2013).
- ⁷⁵ F. Wilczek and A. Zee, *Phys. Rev. Lett.* **51**, 2250 (1983).